Electronic Supplementary Information

Implementation of an Open Source Algorithm for Particle Recognition and Morphological Characterization for Microplastic Analysis by Means of Raman Microspectroscopy

Philipp M. Anger[1], Leonhard Prechtl[1], Martin Elsner, Reinhard Niessner and Natalia P. Ivleva

Institute of Hydrochemistry, Chair of Analytical Chemistry and Water Chemistry, Technical University of Munich, Marchioninistr. 17, 81377 Munich/DE

[1]shared first authorship

*Corresponding Author: Natalia P. Ivleva, natalia.ivleva@tum.de

Email addresses: Philipp M. Anger – p.anger@tum.de; Leonhard Prechtl – leonhard.prechtl@tum.de; Martin Elsner – m.elsner@tum.de; Reinhard Niessner reinhard.niessner@ch.tum.de;

In the Electronic Supplementary Information (ESI) we present further information to clarify our statements made in the main manuscript. In Figure S1 we display the Euclidian distance map of figure 2 in the main manuscript. A magnified section of Figure 2e from the main manuscript is shown in Figure S2. From Figure S3 to Figure S20 exemplary processed images are displayed.

Euclidian Distance Map

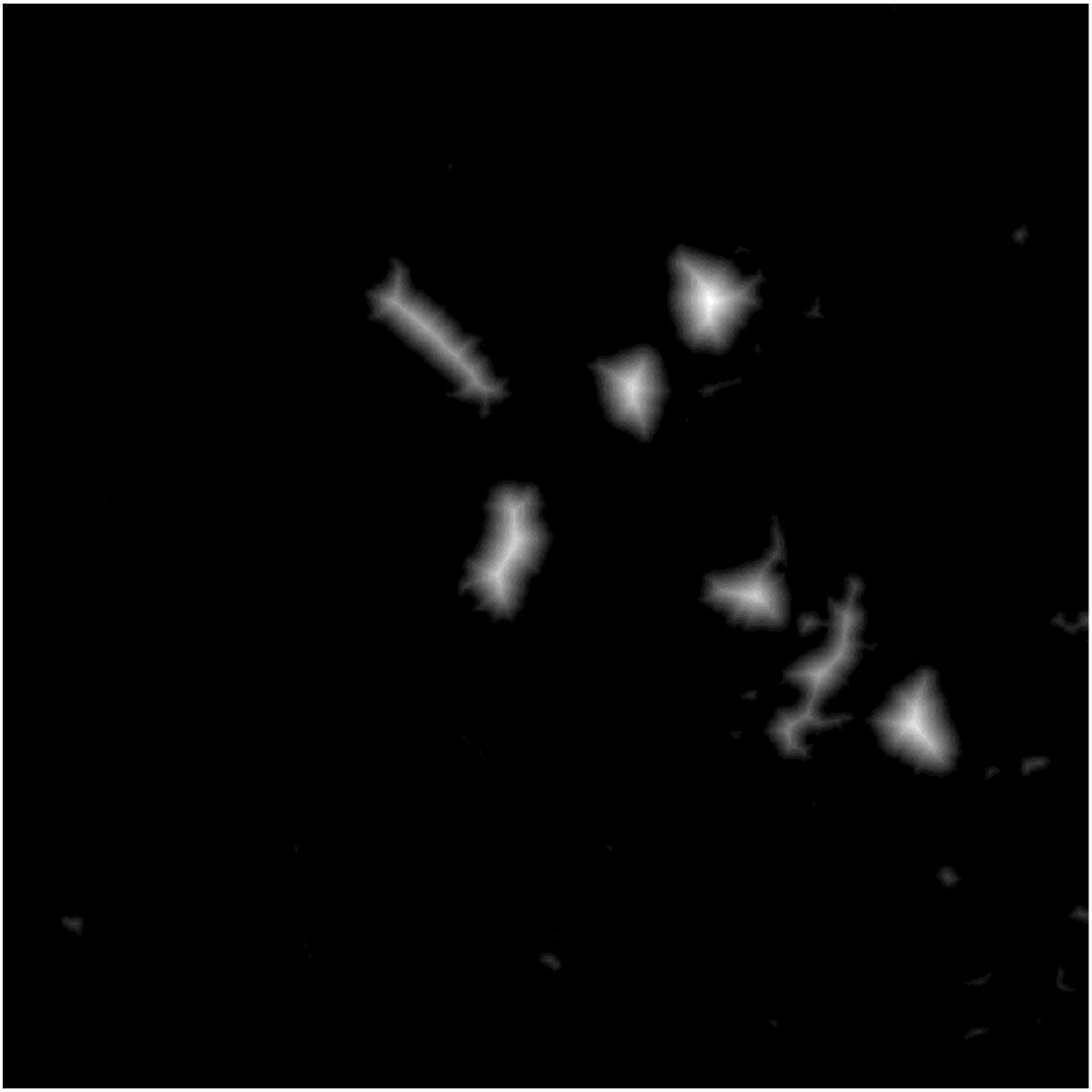

Figure S1: Euclidian distance Map created from fig 2 of the main manuscript.

Magnified section of figure 2e of the main manuscript

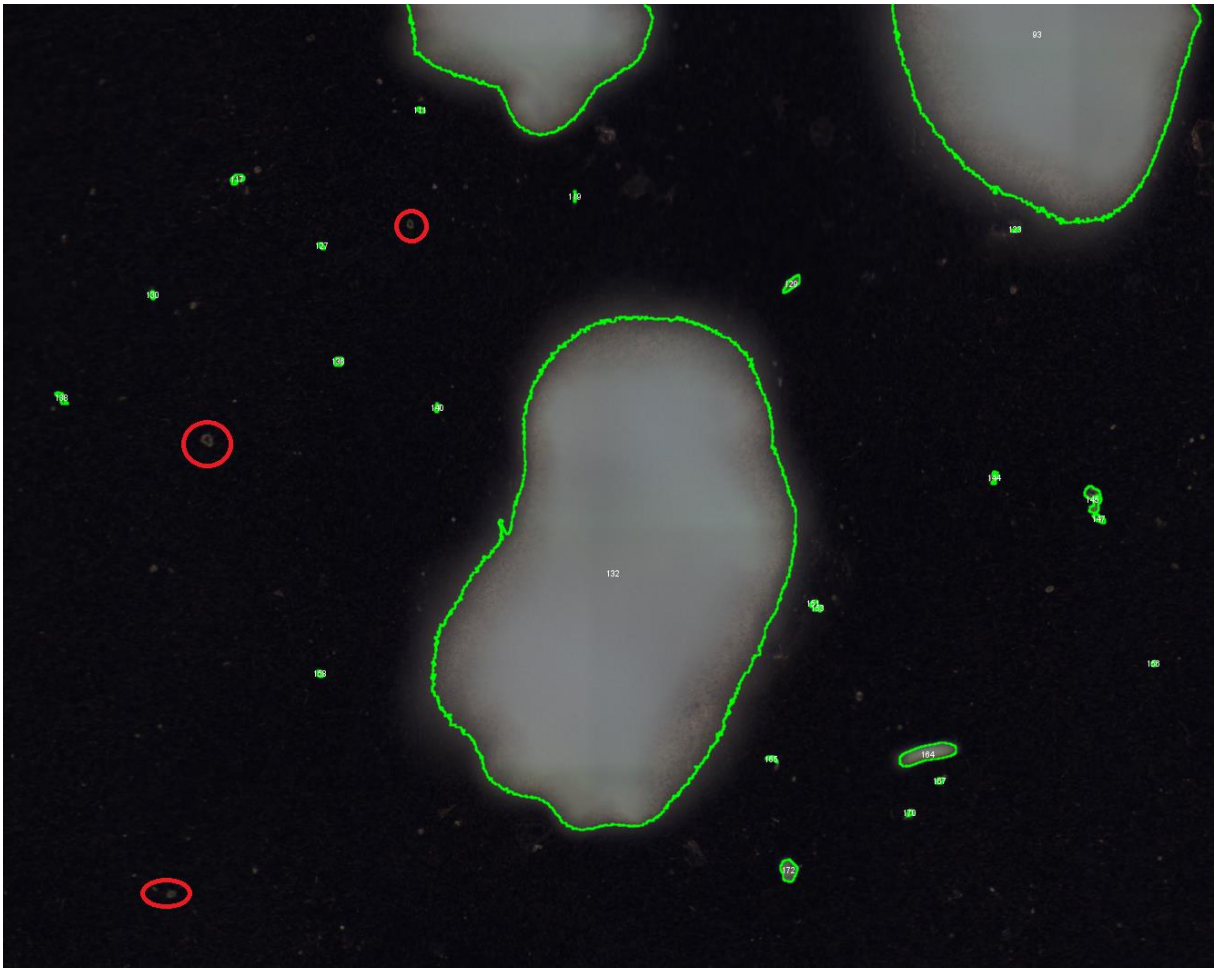

Figure S2: Magnified section of Figure 2e from the main manuscript. Red encircled particles have not been found by the algorithm due to low intensity values of corresponding pixel. Green encircled particles are particles found by the algorithm.

Examples of processed images from published data

The processed images are taken from original publications and except for some pictures where the scales where masked, the images where processed with our Open Source program without further editing. All figures follow the same scheme: Left – original image; middle – processed image without watershed; right – processed image with watershed;

All images but one were processed with default values:

protocol – Single Image

min. pixels = 20 (5 for Figure S18**Fehler! Verweisquelle konnte nicht gefunden werden.**)

min. size / µm = 0

max. size / µm = 100 000

resolution / px μm^{-1} = 1

The setting for white particles is given for every figure.

The comparison of the results of the algorithm and the human expert yields two possible errors: false negatives and false positives. False negatives are worse because these errors describe existing particles which are not found. These errors therefore induce an underestimation of the contaminant under observation. False positives (additional particles or wrong segmentation of existing particles) have the drawback that they induce a longer measurement time and smaller particle sizes. The accordance value in this work gives the accordance of the existing particles (human expert) and the ones the algorithm has found. False positives are subtracted from the overall number of found particles. Thus, every missing particle or false negative leads to an accordance value below 100%.

Accordance = $(N_{algortihm} - N_{false\text{-}positves}) / N_{human\text{-}expert}$

Accordance in % = $((N_{algortihm} - N_{false\text{-}positves}) / N_{human\text{-}expert})*100$

$N_{algorithm}$ = number of particles found by the algorithm

$N_{false\text{-}positives}$ = number of false positives, determined by comparison of particles assigned by human expert and processed image of algorithm

$N_{human\text{-}expert}$ = number of particles found by human expert

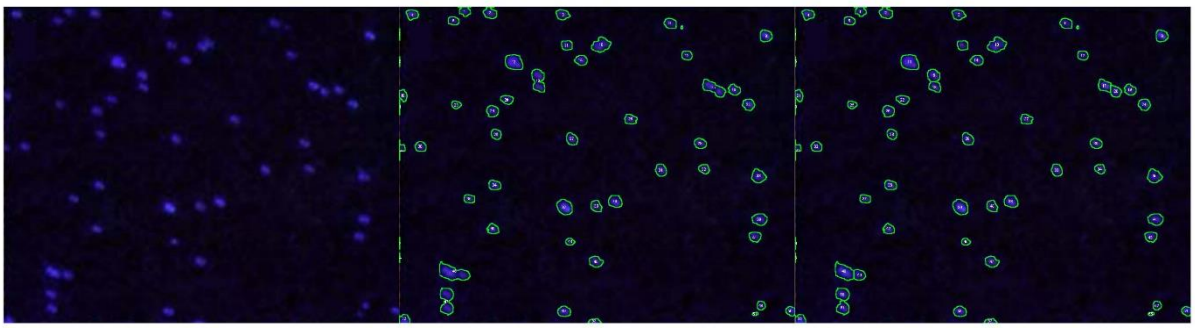

Figure S3: Image from Ossmann et al. [1] Figure 4f; "white particles" were looked for.

Table S1: Accuracy or validity of images from Figure S3.

	# particles	Accordance / %	False negatives	False positives
Human Expert	50			
Otsu	53	92.0	4	7
Otsu + watershed	57	100	0	7

Table S2: Reliability or precision of images from Figure S3.

	# particles	Accordance / %	False negatives	False positives
Otsu	53			
Otsu rotation 90°	53	100	0	0
Otsu vertical flip	53	100	0	0
	# particles	Accordance / %	False negatives	False positives
Otsu + watershed	57			
Otsu + watershed rotation 90°	57	100	0	0
Otsu + watershed vertical flip	57	100	0	0

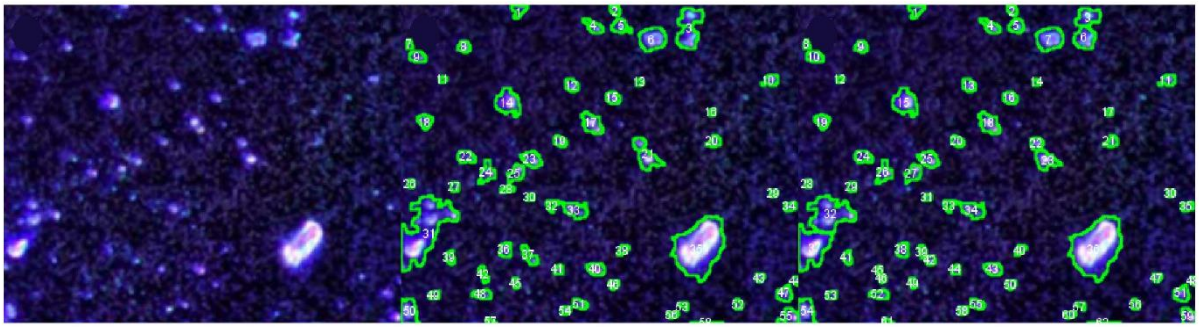

Figure S4: Image from Ossmann et al. [1] Figure 4g; "white particles" were looked for.

Table S3: Accuracy or validity of images from Figure S4.

	# particles	Accordance / %	False negatives	False positives
Human Expert	53			
Otsu	58	79.2	11	16
Otsu + watershed	62	83.0	9	18

Table S4: Reliability or precision of images from Figure S4.

	# particles	Accordance / %	False negatives	False positives
Otsu	58			
Otsu rotation 90°	58	100	0	0
Otsu vertical flip	58	100	0	0
	# particles	Accordance / %	False negatives	False positives
Otsu + watershed	62			
Otsu + watershed rotation 90°	63	100	0	1
Otsu + watershed vertical flip	63	100	0	1

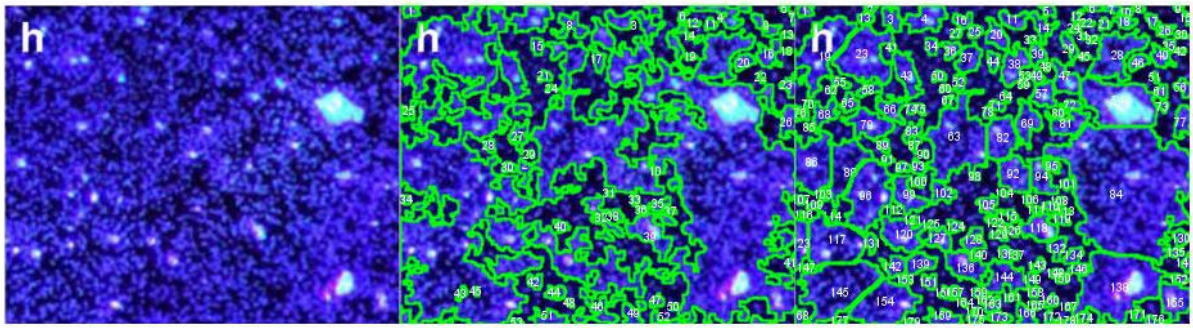

Figure S5: Image from Ossmann et al. [1] Figure 4h; "white particles" were looked for.

In

Figure *S5* a lot of false positives are created due to the over-illumination of this sample. Pores of the filter "glow" and are thereby mistaken as particles or parts of particles. Therefore, this image was not further evaluated.

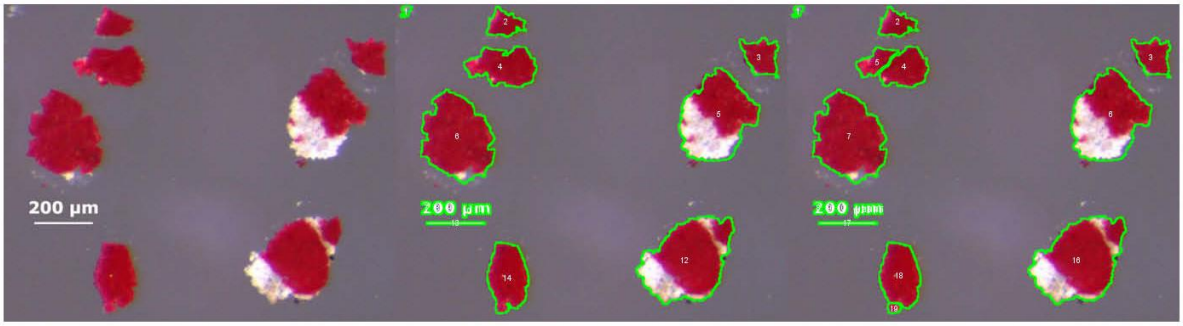

Figure S6: Image from Käppler et al. 2018 [2], Figure 1c; "white particles" were looked for.

Table S5: Accuracy or validity of images from Figure S6.

	# particles	Accordance / %	False negatives	False positives
Human Expert	8			
Otsu	8	100	0	0
Otsu + watershed	10	100	0	2

Table S6: Reliability or precision of images from Figure S6.

	# particles	Accordance / %	False negatives	False positives
Otsu	8			
Otsu vertical flip	8	100	0	0
	# particles	Accordance / %	False negatives	False positives
Otsu + watershed	10			
Otsu + watershed vertical flip	10	100	0	0

90° values are missing for Figure S6, due to a limitation in length/width ratio that can be processed by our open source program. However, all other images showed no deviation by 90° rotation. Therefore, we recommend to rotate images with unsuitable length/width ratios.

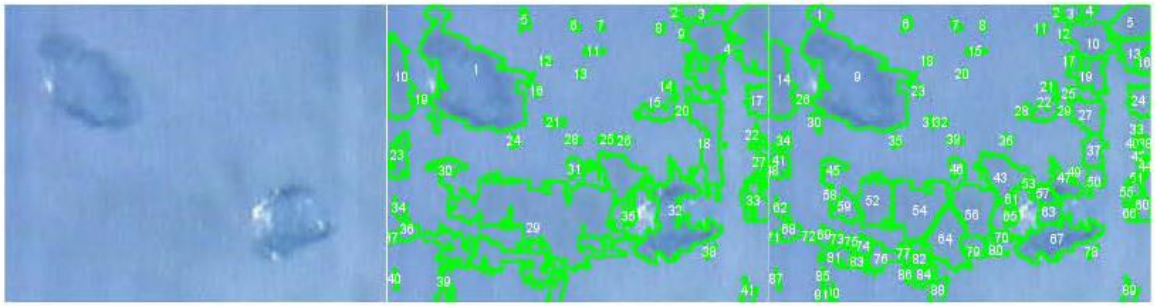

*Figure S7: Image reproduced from Löder et al. [3] Figure 3j, with permission from CSIRO Publishing; "**dark** particles" were looked for.*

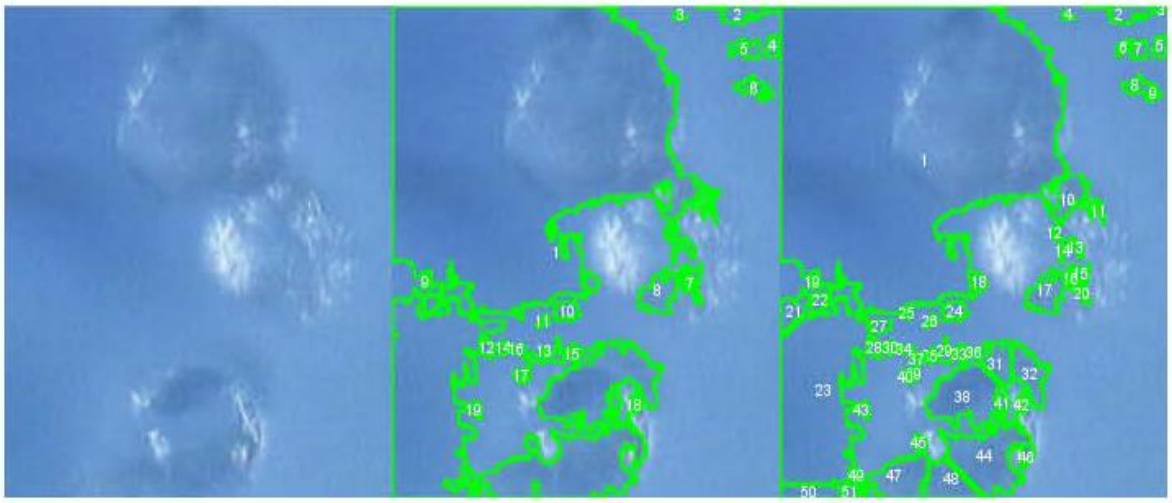

*Figure S8: Image reproduced from Löder et al. [3] Figure 3d, with permission from CSIRO Publishing; "**dark** particles" were looked for.*

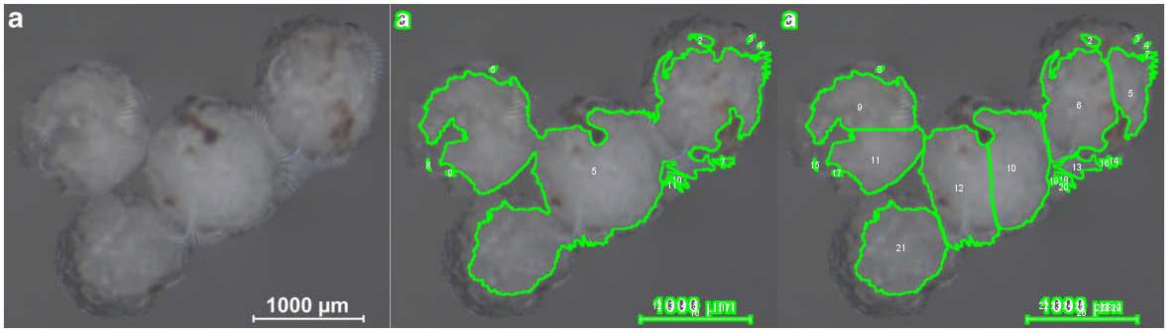

Figure S9: Image from Käppler et al. 2016 [4] Figure 1a; "white particles" were looked for.

Table S7: Accuracy or validity of images from Figure S9.

	# particles	Accordance / %	False negatives	False positives
Human Expert	4			
Otsu	11	75.0	1	8
Otsu + watershed	20	100	0	16

Table S8: Reliability or precision of images from Figure S9.

	# particles	Accordance / %	False negatives	False positives
Otsu	11			
Otsu vertical flip	11	100	0	0
	# particles	Accordance / %	False negatives	False positives
Otsu + watershed	20			
Otsu + watershed vertical flip	20	100	0	0

90° values are missing for Figure S9 due to a limitation in length/width ratio that can be processed by our open source program. However, all other images showed no deviation by 90° rotation. Therefore, we recommend to rotate images with unsuitable length/width ratios.

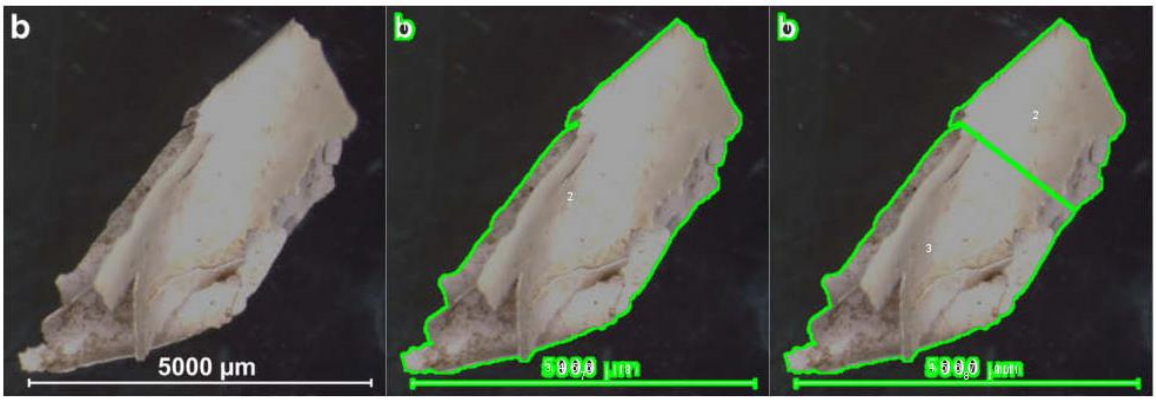

Figure S10: Image from Käppler et al. 2016 [4] Figure 1b; "white particles" were looked for.

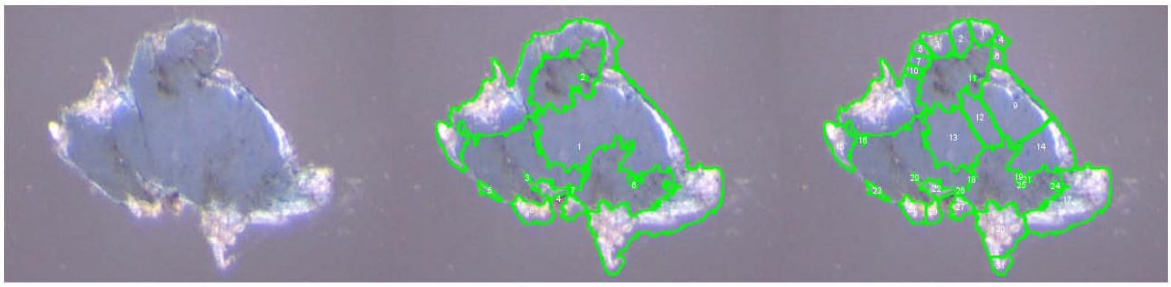

Figure S11: Image from Käppler et al. 2018 [2], Figure 1a; "white particles" were looked for.

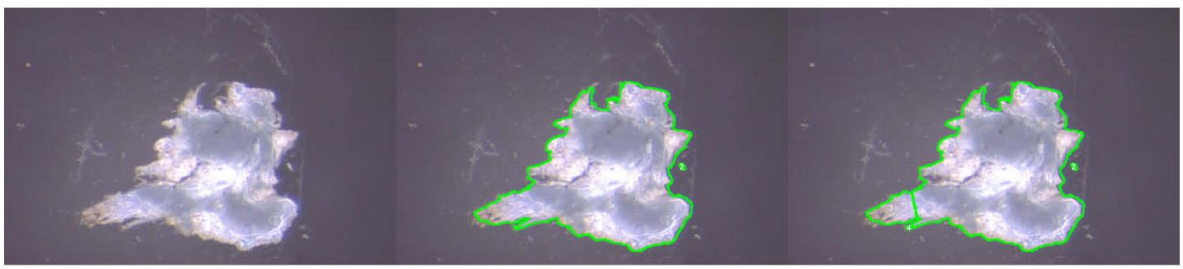

Figure S12: Image from Käppler et al. 2018 [2], Figure 1b; "white particles" were looked for.

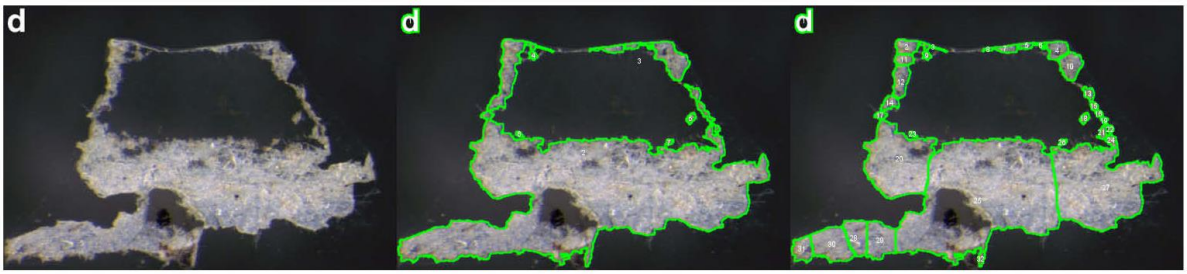

Figure S13: Image from Käppler et al. 2018 [2], Figure 1d; "white particles" were looked for.

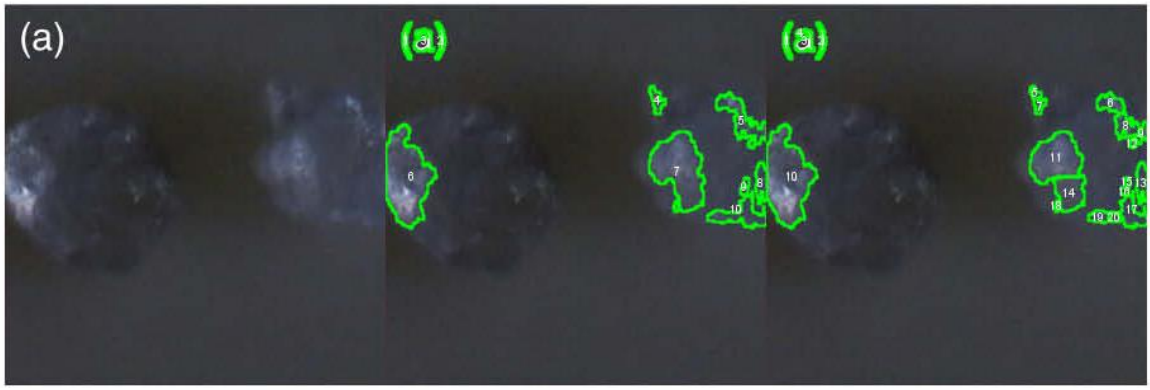

Figure S14: Image reproduced from Löder et al. [3] Figure 3a, with permission from CSIRO Publishing; "white particles" were looked for.

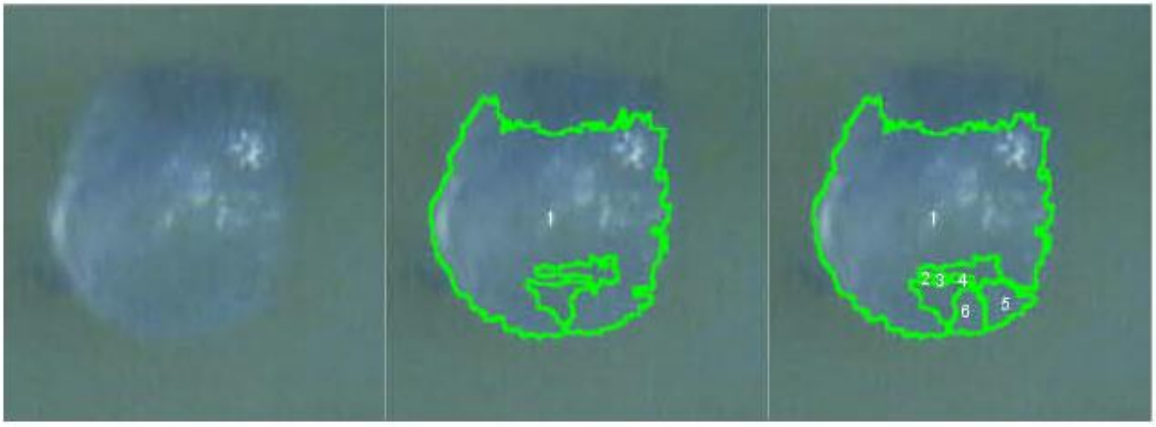

Figure S15: Image reproduced from Löder et al. [3] Figure 3g, with permission from CSIRO Publishing; "white particles" were looked for.

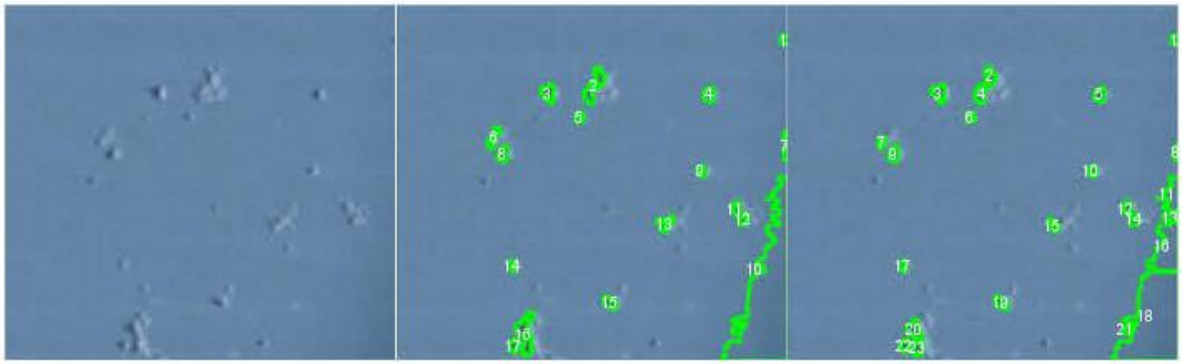

Figure S16: Image reproduced from Löder et al. [3] Figure 9a, with permission from CSIRO Publishing; "white particles" were looked for.

Table S9: Accuracy or validity of images from Figure S16.

	# particles	Accordance / %	False negatives	False positives
Human Expert	20			
Otsu	17	65.0%	7	4
Otsu + watershed	23	65.0%	7	10

Table S10: Reliability or precision of images from Figure S16.

	# particles	Accordance / %	False negatives	False positives
Otsu	17			
Otsu rotation 90°	17	100	0	0
Otsu vertical flip	17	100	0	0
	# particles	Accordance / %	False negatives	False positives
Otsu + watershed	23			
Otsu + watershed rotation 90°	23	100	0	0
Otsu + watershed vertical flip	23	100	0	0

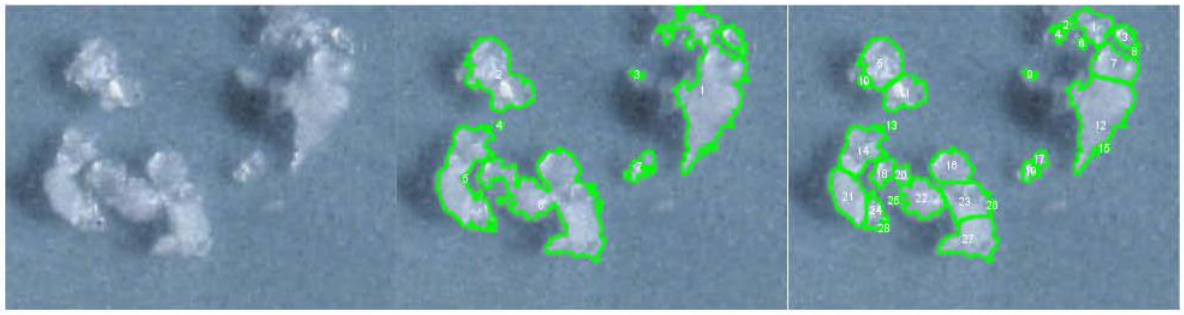

Figure S17: Image reproduced from Löder et al. [3] Figure 9d with, permission from CSIRO Publishing; "white particles" were looked for.

Table S11: Accuracy or validity of images from Figure S17.

	# particles	Accordance / %	False negatives	False positives
Human Expert	10			
Otsu	7	60	4	1
Otsu + watershed	28	100	0	18

Table S12: Reliability or precision of images from Figure S17.

	# particles	Accordance / %	False negatives	False positives
Otsu	7			
Otsu rotation 90°	7	100	0	0
Otsu vertical flip	7	100	0	0
	# particles	Accordance / %	False negatives	False positives
Otsu + watershed	28			
Otsu + watershed rotation 90°	28	100	0	0
Otsu + watershed vertical flip	28	100	0	0

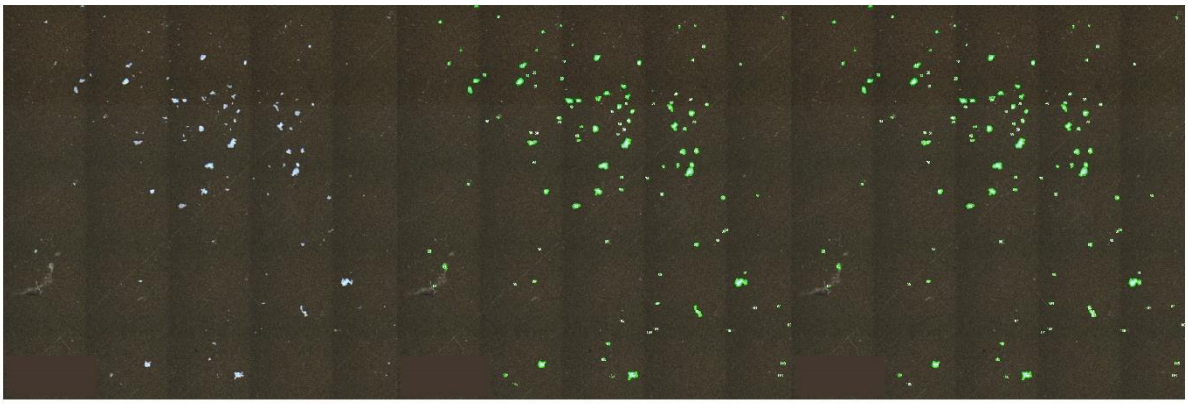

Figure S18:Exemplary image of polystyrene particles on a gold filter under dark field illumination. "white particles" were looked for.

This image is the only one with very small particles compared to the overall image size. Therefore, the min. pixels was set to 5.

Table S13: Accuracy or validity of images from Figure S18.

	# particles	Accordance / %	False negatives	False positives
Human Expert	127			
Otsu	115	90.6	12	0
Otsu + watershed	120	92.9	9	2

Table S14: Reliability or precision of images from Figure S18.

	# particles	Accordance / %	False negatives	False positives
Otsu	115			
Otsu rotation 90°	115	100	0	0
Otsu vertical flip	115	100	0	0
	# particles	Accordance / %	False negatives	False positives
Otsu + watershed	120			
Otsu + watershed rotation 90°	120	100	0	0
Otsu + watershed vertical flip	120	100	0	0

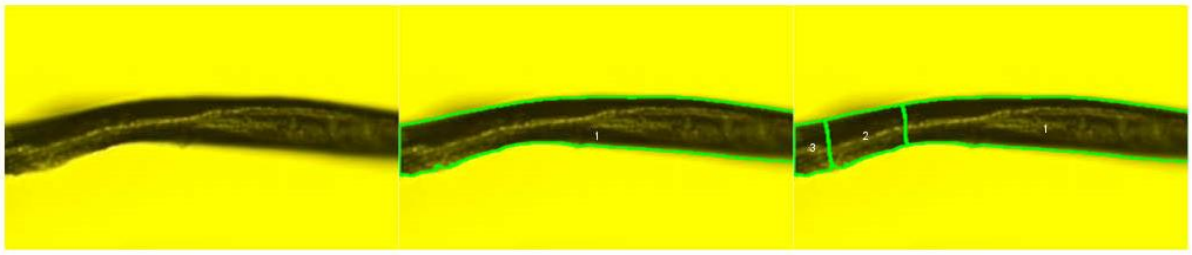

*Figure S19: Image from Käppler et al. 2016 [4] Figure 1d; "**dark** particles" were looked for.*

*Figure S20: Exemplary image of a polystyrene fibre on a polycarbonate filter under bright field illumination. "**dark** particles" were looked for.*

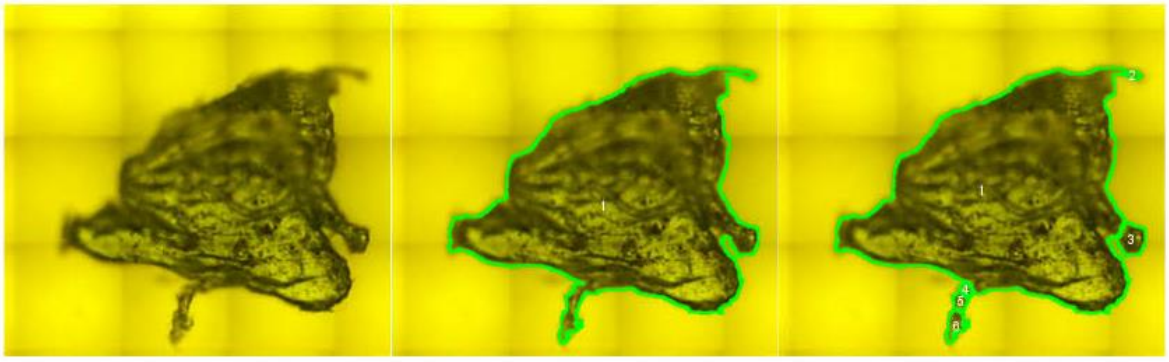

*Figure S21: Image from Käppler et al. 2016 [4] Figure 1c; "**dark** particles" were looked for.*

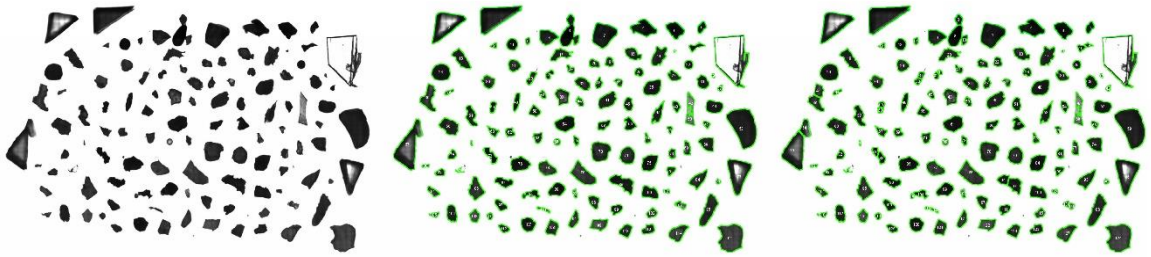

*Figure S22: Image from Frère et al. [5] Figure 3; "**dark** particles" were looked for.*

Table S15: Accuracy or validity of images from Figure S22.

	# particles	Accordance / %	False negatives	False positives
Human Expert	119			
Otsu	114	95.0%	6	1
Otsu + watershed	127	96.6%	4	12

Table S16: Reliability or precision of images from Figure S22.

	# particles	Accordance / %	False negatives	False positives
Otsu	114			
Otsu vertical flip	114	100	0	0
	# particles	Accordance / %	False negatives	False positives
Otsu + watershed	127			
Otsu + watershed vertical flip	127	100	0	0

90° values are missing for Figure S22, due to a limitation in length/width ratio that can be processed by the open source program. However, all other images showed no deviation by 90° rotation. Therefore, we recommend to rotate images with unsuitable length/width ratios.

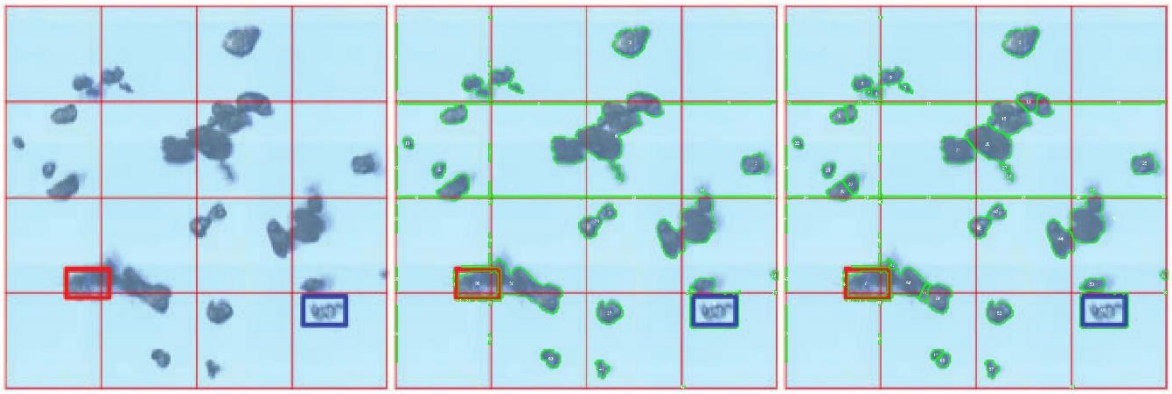

*Figure S23: Image reproduced from Löder et al. [3] Figure 1b, with permission from CSIRO Publishing; "**dark** particles" were looked for.*

Table S17: Accuracy or validity of images from Figure S23.

	# particles	Accordance / %	False negatives	False positives
Human Expert	30			
Otsu	42	60.0%	12	24
Otsu + watershed	68	93.3%	2	40

Table S18: Reliability or precision of images from Figure S23.

	# particles	Accordance / %	False negatives	False positives
Otsu	42			
Otsu rotation 90°	42	100	0	0
Otsu vertical flip	42	100	0	0
	# particles	Accordance / %	False negatives	False positives
Otsu + watershed	68			
Otsu + watershed rotation 90°	68	100	0	0
Otsu + watershed vertical flip	68	100	0	0

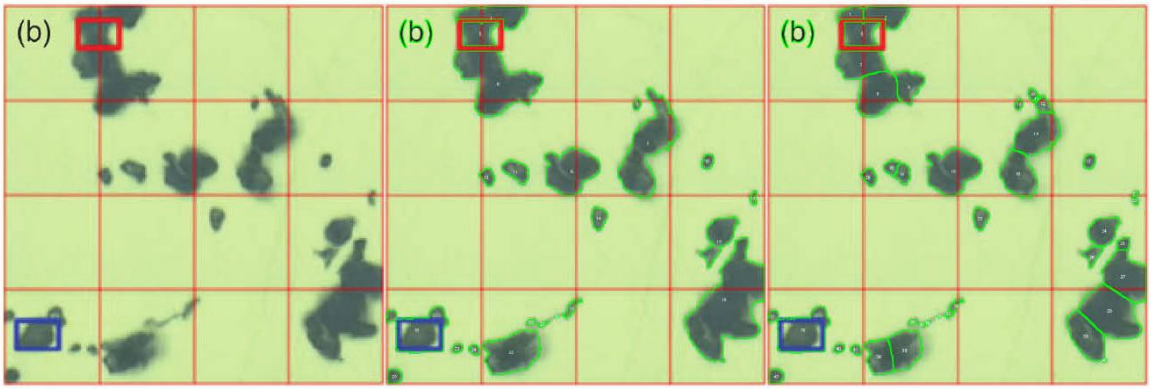

*Figure S24: Image reproduced from Löder et al. [3] Figure 2b, with permission from CSIRO Publishing; "**dark** particles" were looked for.*

Table S19: Accuracy or validity of images from Figure S24.

	# particles	Accordance / %	False negatives	False positives
Human Expert	27			
Otsu	22	70.4%	8	3
Otsu + watershed	40	92.6%	2	15

Table S20: Reliability or precision of images from Figure S24.

	# particles	Accordance / %	False negatives	False positives
Otsu	22			
Otsu rotation 90°	22	100	0	0
Otsu vertical flip	22	100	0	0
	# particles	Accordance / %	False negatives	False positives
Otsu + watershed	40			
Otsu + watershed rotation 90°	40	100	0	0
Otsu + watershed vertical flip	40	100	0	0

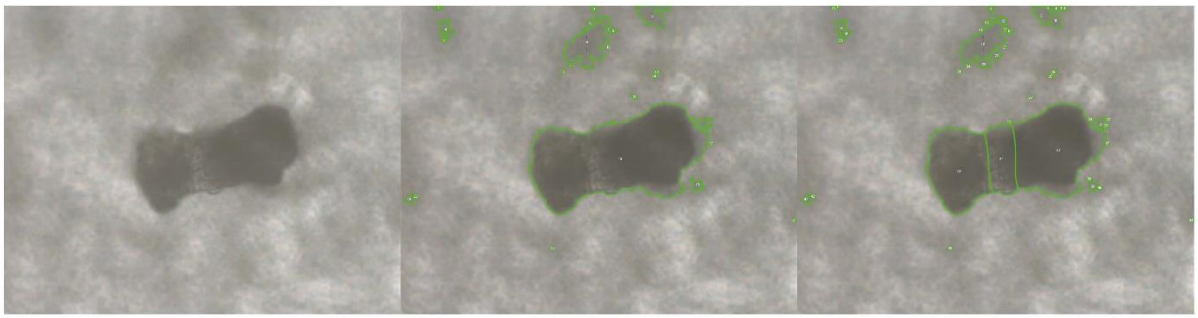

*Figure S25: Image from Domogalla-Urbansky and Anger et al. [6] Figure 2c; "**dark** particles" were looked for.*

References

1. Ossmann BE, Sarau G, Schmitt SW, Holtmannspotter H, Christiansen SH, Dicke W. Development of an optimal filter substrate for the identification of small microplastic particles in food by micro-Raman spectroscopy. Anal Bioanal Chem. 2017. doi:10.1007/s00216-017-0358-y.
2. Kappler A, Fischer M, Scholz-Bottcher BM, Oberbeckmann S, Labrenz M, Fischer D et al. Comparison of mu-ATR-FTIR spectroscopy and py-GCMS as identification tools for microplastic particles and fibers isolated from river sediments. Anal Bioanal Chem. 2018. doi:10.1007/s00216-018-1185-5.
3. Löder MGJ, Kuczera M, Mintenig S, Lorenz C, Gerdts G. Focal Plane Array Detector-Based Micro-Fourier-Transform Infrared Imaging for the Analysis of Microplastics in Environmental Samples. Environ Chem. 2015;12(5):563-81. doi:10.1071/en14205.
4. Käppler A, Fischer D, Oberbeckmann S, Schernewski G, Labrenz M, Eichhorn KJ et al. Analysis of environmental microplastics by vibrational microspectroscopy: FTIR, Raman or both? Anal Bioanal Chem. 2016;408(29):8377-91. doi:10.1007/s00216-016-9956-3.
5. Frère L, Paul-Pont I, Moreau J, Soudant P, Lambert C, Huvet A et al. A semi-automated Raman micro-spectroscopy method for morphological and chemical characterizations of microplastic litter. Mar Pollut Bull. 2016;113(1):461-8. doi:https://doi.org/10.1016/j.marpolbul.2016.10.051.
6. Domogalla-Urbansky J, Anger PM, Ferling H, Rager F, Wiesheu AC, Niessner R et al. Raman microspectroscopic identification of microplastic particles in freshwater bivalves (Unio pictorum) exposed to sewage treatment plant effluents under different exposure scenarios. Environmental science and pollution research international. 2018. doi:10.1007/s11356-018-3609-3.